1 High Energy Nuclear Physics

> *Three quarks for Muster Mark!*
> *Sure he has not got much of a bark*
> *And sure any he has it's all beside the mark.*
>
> **— James Joyce**
> (Finnegans Wake)

According to cosmological theories, in its early stages the Universe was extremely hot and dense. In the first few microseconds, the energy densisty was so high that hadrons could not be formed and their foundamental constituents were in a deconfined state. When the energy density has decreased enough, a phase transition led to the formation of the ordinary matter.

High Energy Nuclear Physics (HENP) investigates the hot and dense nuclear matter and the properties of its phase transition into ordinary matter through the study of ultra-relativistic heavy-ion collisions. The aim is to improve our understandig of the behaviour of the matter in extereme conditions and of the Universe at the beginning of its life.

1.1 QCD: the theory of the Strong Interaction

In 1964 M. Gell-Mann and G. Zweig proposed independently a model that could explain the existence of the great variety of hadrons discovered in the 1950s and 1960s [1–3]. This model, known as the Static Quark Model, was based on the assumption that hadrons are not fundamental particles, but they are composed states of elementary constituents called quarks. In this way it was possible to explain the large number of particles observed and their properties, which showed some sort of pattern, in term of constituents properties. Furthermore, thanks to the Static Quark Model, it was possible predict new hadrons (e.g. Ω^-) and to explain why certain particles don't exist (e.g. baryons with $S = +1$). However, this model could not deal with many questions: why there is no evidence of free quarks? What hold quarks together in a hadron? Why the Δ^{++} baryon exists despite is forbidden by Pauli's Principle? In order to answer these questions it was necessary to introduce

a new quantum number the colour [4]. The introduction of the colour led to the formulation of a quantum field theory for the Strong Interaction, inspired by the Quantum Electrodynamics (QED), the Quantum Chromodynamics (QCD).

The QCD is a non-Abelian quantum gauge theory, based on the invariance under local $\mathrm{SU}(3)_c$ group transformations. The choice of this particular symmetry group is due to the hypothesis that the colour comes in three different states: red, blue and green. The local invariance under $\mathrm{SU}(3)_c$ implies the existence of 8 massless gauge bosons mediators of the colour interaction, called gluons [5]. Therefore the QCD Lagrangian can be written as:

$$\mathcal{L}_{\mathrm{QCD}} = \bar{\psi}_i(i(\gamma^\mu D_\mu)_{ij} - m\,\delta_{ij})\psi_j - \frac{1}{4}G^a_{\mu\nu}G^{\mu\nu}_a \tag{1.1}$$

where the first term is related to quarks fields while the second is releted to gluons fields. In the first term $\psi_i(x)$ represents the quarks fields expressed in the fundamental representation of $\mathrm{SU}(3)_c$, while D_μ is the covariant derivative, defined as:

$$D_\mu = \partial_\mu - ig_s A^a_\mu \lambda_a. \tag{1.2}$$

In this derivarives shows up the coupling constant for the Strong Interaction g_s, the Gell-Mann matrices λ_α which gives a representation of the generators of $\mathrm{SU}(3)_c$ symmetry group, and the gluon field $A(x)$. This first term of the QCD Lagrangian represents the quarks-gluons interaction via a QED-like vertex.

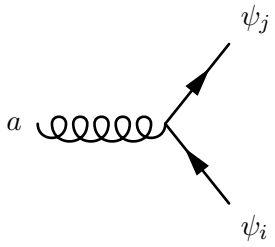

Fig. 1.1: Feynman diagram for the gluon-quarks interaction.

The second term of the Lagrangian $G^a_{\mu\nu}$ represents the gauge invariant gluon field strength tensor, and can be written as:

$$G^a_{\mu\nu} = \partial_\mu A^a_\nu - \partial_\nu A^a_\mu + g_s f^{abc} A^b_\mu A^c_\nu. \tag{1.3}$$

In this tensor $g_s f^{abc} A^b_\mu A^c_\nu$ is the non-Abelian part of the theory, which implies the self-interactions among gluons. This interactions have resulted from the fact that gluons carry a colour and an anti-colour charge, so they can interact among themselves. Therefore in addition to the QED-like vertex, in the QCD, 3 gluons and 4

gluons vertex are allowed at the tree level. The existence of the gluons vertex allows to have gluons loops.

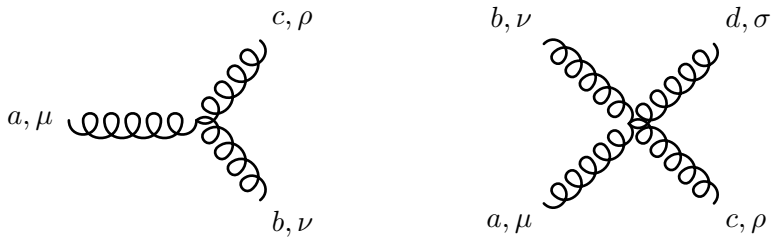

Fig. 1.2: Feynman diagrams for the gluon-gluon interactions at the tree level.

In the renormalization process of the theory, the non-Abelian nature of the QCD brings to the so-called *anti-screening* in colour interaction. Adding loop corrections to the gluons propagator, gluons loops contribute to the sum with opposite sign respect to the quarks loops. Therefore, in addition to the QED-like *screening* effect, there is an *anti-screening* effect due to gluons loops. As a result, the QCD shows up its specific features, *asymptotic freedom* and *confinement*.

Setting $\alpha_s = g_s^2/4\pi$ strong coupling constant can be written as [6]:

$$\alpha_s(Q^2) = \frac{\alpha_s(\mu^2)}{1 + \alpha_s(\mu^2)(33 - 2\,n_f)\ln(Q^2/\mu^2)} \tag{1.4}$$

where n_f is the number of quark families and μ is the renormalization scale of the theory. For high transferred momenta α_s goes to zero and the QCD becomes a free theory and this regime is called *asymptotic freedom*. At low Q^2 the Strong copuling diverges, forcing quarks to be strongly bound in hadrons: the so-called *confinement* regime. This behaviour of the QCD copuling constant has been confirmed by experimental results over the years as shown in Figure 1.3. The equation 1.4 can be rewritten fixing the energy scale:

$$\alpha_s(Q^2) = \frac{12\pi}{(33 - 2\,n_f)\ln(Q^2/\Lambda_{\mathrm{QCD}})} \tag{1.5}$$

where Λ_{QCD} is the renormalization scale of QCD (typically ≈ 200 MeV).

In QCD the perturbative approach used to calculate the elements of the scattering matrix (pQCD), is possible only for high Q^2 processes ($Q^2 \gg \mu^2$, thus $\alpha_s \ll 1$). As already mentioned, in low transferred momentum processes α_s diverges. Therefore, is impossible to express the elements of the scattering matrix in terms of power series expansion of the Strong copuling constant. In this regime it is still possible to evaluate the Green's functions of the QCD Lagrangian on a space-time lattice with spacing a, as proposed in 1974 by Wilson [7]. With this method, called lattice QCD

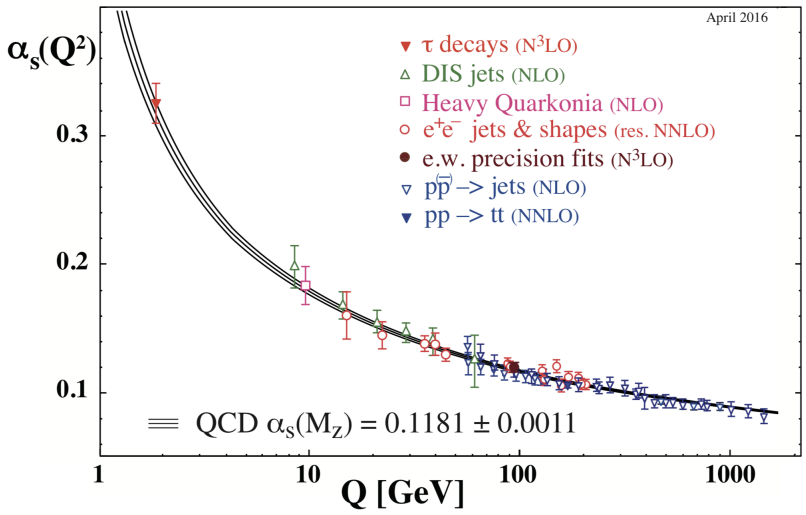

Fig. 1.3: Summary of measurements of α_s as a function of the energy scale Q [6].

(lQCD) is possible to extrapolate to the continuum ($a \to 0$) and get results to be compared with the experiments.

1.2 States of hadronic matter

One of the interesting consequences of the running copuling constant is the possibility of having different states of the hadronic matter. The state is essentially determined by the mean transferred momentum in the interactions which define the value of α_s. A system with low mean transferred momentum it is in the *confinement* regime, therefore quarks and gluons are required to be confined in hadrons. Otherwise in high mean transferred momentum systems, the *asymptotic freedom* regime allows the formation of a plasma where quarks and gluons are essentially free. This state of matter is called Quark Gluon Plasma (QGP) and is supposed that the universe was in this state in the first microseconds after the Big Bang. One of the main goals of the HENP is the study of the phase transitions between the different states of the hadronic matter.

Considering a system with finite dimensions, composed by hadronic matter, can be useful to describe it using thermodinamical variables like temperature (T) and chemical potential (μ). In this specific framework the chemical potential is interpreted as the energy required to create a baryonic state and it is called baryon chemical potential (μ_B). Figure 1.4 shows the phase diagram of the QCD matter predicted by the theory and the values of temperature T and baryon chemical potential (μ_B) which are accessible experimentally in high energy heavy ion collisions.

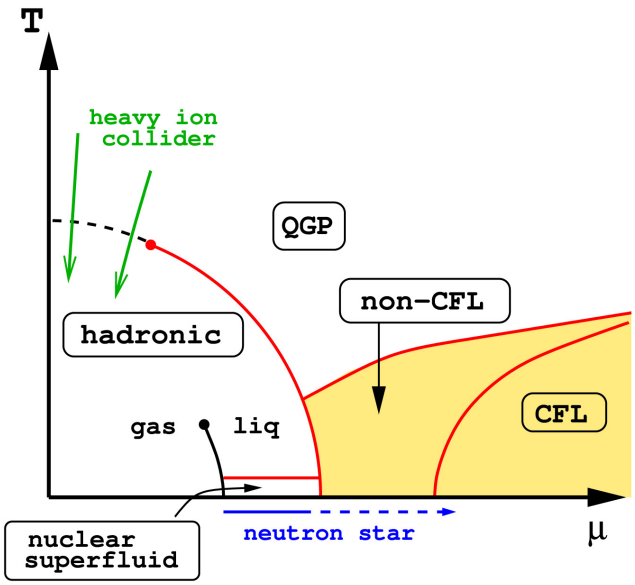

Fig. 1.4: Schematic representation of the nuclear matter phase diagram from [8]. QGP refers to the Quark Gluon Plasma state, CFL (Colour-Flavour Locked) corresponds to the colour superconducting phase that is present in systems with high baryon chemical potential. The green arrows represent the phase space investigated by collider experiments at the Relativistic Heavy Ion Collider (RHIC) and at the LHC.

The origin of the diagram (T$=\mu_B=0$ GeV) corresponds to the QCD vacuum. At T$=0$ GeV, μ_B is the energy required to create a baryonic state, therefore ordinary matter (proton, neutrons and nuclei) sits around 1 GeV on the μ_B axis. Along the μ_B axis lies a phase transition to a state, the Color Superconducting Phase, that has been hypothesised to be present in matter at high density, e.g. in the core of neutron stars [9]. Along the T axis, where $\mu_B = 0$, there is a phase transition when T $\gg \Lambda_{\mathrm{QCD}}$. At this temperatures the average momentum exchange between quarks and gluons is so high that they reach the *asymptotic freedom*, hence they are no longer confined in colour singlets states. In these conditions they constitute a plasma of free coloured partons, similar to the primordial universe: the aforementioned QGP.

The order of the phase transition is determined by the behaviour of the derivatives of the free energy of the system with respect to time. It basically describes how fast the free energy varies in a neighbourhood of the transition temperature. A first order transitions takes place when a latent heat is present, leading to a discontinuous free energy first derivatives and variation of entropy. If no latent heat is involved in the process, occours a second order transition. The free energy first derivative is continuous, while derivatives of higher than first order of the free energy are discontinuous. When the transition occours with a continuous behaviour of the free energy and its derivatives, it is called a *crossover* transition. In $\mu_B = 0$ conditions, the transition from hadron gas to the QGP takes place when T ≈ 150 MeV with a *crossover* transition.

1.3 Heavy Ion Collisions

The QCD phase diagram is derived by theories and models, but their predictions are difficult to test. For the T ≈ 0 GeV and high μ_B region, important suggestions can come from astronomic observations of neutron stars. For high T regions, instead, the only known way to cross the phase boundary between ordinary hadronic matter and QGP is by colliding ultrarelativistic heavy ions in the laboratory.

The journey of the High Energy Nuclear Physics started in the '70 at the Lawrence Berkeley National Laboratory where the first experiments on heavy ions collisions (HIC) was performed at modestly relativistic conditions (≈ 2 GeV/nucleon). In 1986, two HIC experiments started simultaneously at the Super Proton Syncrotron (SPS) at CERN and at the Alternate Gradient Syncrotron (AGS) at Brookhaven, colliding O ions at fixed target at higher energies. Nowdays the two main hadron colliders active with an HIC program and dedicated experiments are the Relativistic Heavy Ion Collider (RHIC) at the Brookhaven National Laboratory (BNL) and the Large Hadron Collider (LHC) at CERN.

1.3.1 The "Little Bang" at the LHC

Atomic nuclei are composite systems of nucleons with finite dimensions. When they collide at ultrarelativistic energies the problem of the description of the collision, that can be very complex, arises. The Glauber Model [10] is a semi-classical model describing nucleus–nucleus interaction in terms of nucleon–nucleon (NN) interactions. The Glauber Model is based on the assumption of the *optical limit*:

- nucleons are point like and independent inside the nuclei;
- only hadronic interactions are considered: protons and neutrons cannot be distinguished;
- the collision does not deflect colliding nucleons: they travel in a straight line;
- the cross section for an elementary nucleon-nucleon interaction is constant during the whole process.

With this assumption the Glauber Model allows a quantitative calculation of the interaction probability, the number of elementary NN collisions (N_{coll}), the number of the partecipants nucleons (N_{part}) and extension of the overlap region. These quantities are expressed in terms of the impact parameter $\vec{b}$, which characterizes the

collisions geometry. A direct experimental measurement of the impact parameter is precluded and the same goes for N_{coll} and N_{part}. However, the Glauber Model enables to correlate this variables with measurable quantities such as the total number of particles produced in the collision.

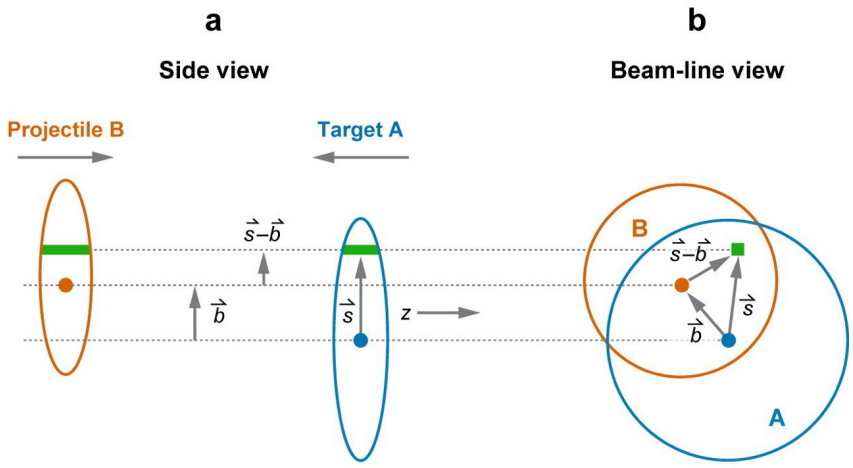

Fig. 1.5: Sketch of the longitudinal and transverse view of an heavy ion collision taken from [10]. In the side view, the colliding nuclei are squeezed to represent the Lorentz boost contraction due to their momentum.

Following the notation introduced in Figure 1.5 the nuclear overlap function for two colliding nuclei (A and B) can be written as:

$$T_{AB}(\vec{b}) = \int T_A(\vec{s})\, T_B(\vec{s}-\vec{b})\, d^2s \tag{1.6}$$

and represents the probability of finding a nucleon in both the colliding nuclei inside the overlap region in the transverse plane. $T_A(\vec{s})$ and $T_B(\vec{s}-\vec{b})$ are the *thickness functions* the A and B nuclei. They represent the probability of finding a nucleon in the unit transverse area located at $\vec{s}$ given the probability per unit volume $\rho(\vec{s},z)$:

$$T(\vec{s}) = \int \rho(\vec{s},z)\, dz\,. \tag{1.7}$$

As assumed, binary only interactions between nucleons are considered and the interaction does not deflect the trajectory of the interacting nucleons. Therefore, each nucleons can participate in more than one binary collision. The probability of having n binary collisions between the nuclei A and B, having A and B nucleons respectively, can be computed using the binomial statistics:

$$P(n,\vec{b}) = \frac{AB!}{n!(AB-n)!}[T_{AB}(\vec{b})\sigma_{inel}]^n[1-T_{AB}(\vec{b})\sigma_{inel}]^{AB-n}. \tag{1.8}$$

From this expression the total inelastic cross section is obtained as a function of the impact parameter integrating the double differential cross section for two colliding nuclei:

$$\frac{d^2\sigma_{inel}^{AB}(b)}{db^2} = \sum_{n=1}^{AB} P(n,b) = 1 - [1 - T_{AB}(\vec{b})\,\sigma_{inel}]^{AB} \tag{1.9}$$

$$\sigma_{inel}^{AB}(b) = \int_0^{\infty} 2\pi\, b\, db\, [1 - [1 - T_{AB}(\vec{b})\,\sigma_{inel}]^{AB}] \tag{1.10}$$

From eq. 1.8, N_{coll} can be derived as a function of the impact parameter summing all the possible numbers of collisions weighted by their own probability and using the definition of the mean of the binomial distribution:

$$\mathrm{N}_{coll}(b) = \sum_{n=1}^{AB} n\, P(n,b) \;= AB\, T_{AB}\, \sigma_{inel}. \tag{1.11}$$

Similarly N_{part} can be obtained by integrating over $\vec{s}$ the contribution of the projectile nucleus and the contribution of the target nucleus as follow:

$$\mathrm{N}_{part}(b) = \int d^2s\, \{A\, T_A(\vec{s})[1-(1-T_B(\vec{b}-\vec{s})\,\sigma_{inel})^B] + B\, T_B(\vec{b}-\vec{s})[1-(1-T_A(\vec{s})\,\sigma_{inel})^A]\} \tag{1.12}$$

In eq. 1.11 and 1.12, $\vec{b}$ has been replaced with its norm as the direction of the vector is relevant for polarised nuclei only.

In spite of its simplicity, the Glauber Model allows to express N_{coll} and N_{part} starting from $\rho(\vec{s})$ and σ_{inel}. The main limitation is the usage of continuous density functions that implies considering discrete physical quantities as continuous.

1.3.2 Space time evolution of Heavy Ion collisions

When two ultrarelativistic atomic nuclei collide, high hadron density and high temperatures are produced in the impact region. In these conditions a long lived and strongly interacting system is created. The evolution of such a system, as well as the characterisation of its properties, is very important to improve our understanding of the Strong interaction. Hence it is one of the main subject of investigation of HI experiments.

The space-time evolution of the system (procede) in different phases. The current view on the evolution is summarized in Figure 1.6.

1. ***t < 0* fm/*c*:** the two atomic nuclei travel in the beam line. In modern accelerators the nuclei are strongly Lorentz contracted in the beam line direction due to their (velocità) vicina aquella della luce (factor of 2700 at the LHC);

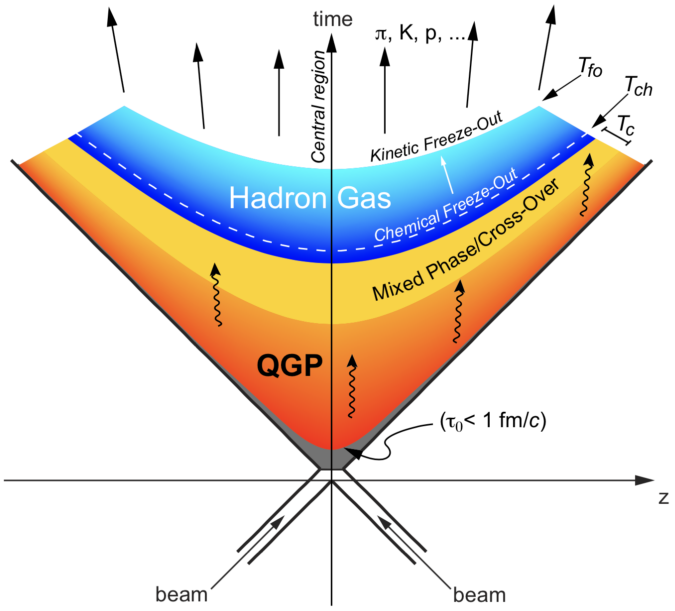

Fig. 1.6: Space-time representation of the evolution of the system created in a central Heavy Ion collision in the mid-rapidity region. The z direction is parallel to the beam line.

2. ***t = 0* fm/*c*:** collision time. The geometry of the collision can be described using the Glauber Model described in the previous section;

3. ***0 < t* $\lesssim$ $\tau_0 \sim$ *1* fm/*c*:** in the early collision stages hard processes (i.e. process with high transferred momentum Q^2) occur between colliding partons. In this phase called *pre–equilibrium*, all the particles with high mass or/and high momentum are produced. In high energy collisions, as at the LHC, the nuclei constituent partons lose their energy in the mid-rapidity[1] region ($y \approx 0$) and then they escape at forward rapidities ($|y| \gg 0$). The escaping valence quarks bring the baryonic potential carried by the colliding nuclei at forward rapidity, vanishing the baryon chemical potential at mid-rapidity. The resulting system is an hot and dense medium. If the energy density is high enough, as at the LHC, a transition to the QGP state is expected. After a short strong parton rescattering phase, the obtained droplet of QGP matter reaches the equilibrium at his proper time τ_0;

4. ***1* $\lesssim$ *t* $\lesssim$ *10* fm/*c*:** the QGP droplet reach the thermal equilibrium and collectively expands under the push of the thermal pressure gradients generated at the system boundaries. Relativistic hydrodynamics models [11] are commonly used to describe the rapid expansion of the QGP matter, providing useful insights to interpret the experimental data. As a consequence of the expantion,

[1]The rapidity is defined, for a particle with four-momentum $p^\mu = (E, \vec{p})$, as $y = \frac{1}{2}\log\left(\frac{E+p_z}{E-p_z}\right)$, with z parallel to the beam direction.

the system cools down and the energy density decreases, transing eventually from the Quark Gluon Plasma phase and ordinary hadronic matter;

5. ***10*** $\lesssim$ ***t*** $\lesssim$ ***15* fm/*c*:** the critical temperature between the two phases is reached. At this temperature the hadronization process starts, leading the system into an interacting *hadron resonance gas*. In this stage, the expansion and the cooling of the system continue, meanwhile elastic and inelastic interactions among the hadrons occour. When the energy density is decreased that much to not allowing inelastic interactions, the relative abundances of different particle species are fixed. The temperature at which the system stops to interact inelastically is called temperature of *chemical freeze-out* T_{ch}. After the *chemical freeze-out* only elastic processes took place, varying the particles momentum. When elestic interactions ends as well, the particles momentum spectra are fixed and this occours at the temperature of *kinetic freeze-out* T_{kin};

6. ***t*** $\gtrsim$ ***15* fm/*c*:** hadrons created in the collision escape the interaction region with no further interactions. This regime is also known as *free hadron stream*.

The particles produced in the collisions and escaped from the interaction region are detected by the experimental apparata carrying informations about the environment in which they have been produced and about the medium in which thay have travelled. In the following it will be shown how properties of the systems and characteristics of its evolution can be inferred by the measurement of particle production spectra and particle correlations.

1.4 Nuclei production in Heavy Ion collisions

The main subject of this thesis is the study of the $d^*(2380)$ dibaryon production at the LHC energies. Except for the deuteron, dibaryons are little known objects. In the next chapter, more details on what dibaryons are and what our understanding is about dibaryons, will be provided.

The (anti-)nuclei are loosely bound objects and it is not trivial how they can emerge from Heavy Ion collisions. The following sections are dedicated to a brief description of the major two classes of models that try to explain the nuclei and anti–nuclei production in HI collisions: the Statistical Hadronisation Models (SHMs) and the Coalescence model [12]. Dibaryons and in particular $d^*(2380)$ – which can be considered as an excited deuteron – should be subject of same production mechanisms as for (anti-)nuclei.

1.4.1 Statistical Hadronisation Models

The Statistical Hadronisation Models (also known as Thermal Models) was successfully developed in order to describe the abundances of different particle species produced in the collision between particles.

The general idea behind these models is that the final state of the interaction is composed by all the particle states compatible with the conservation laws imposed by the underlying theory of interaction (in our case the Standard Model of particle physics). The relative abundance of different particle states is set by the maximisation of the total phase space filled by the system, to which each particle species contributes according to its partition function. These models are of particular interest in HI collisions as the presence of an expanding medium that eventually reaches the thermal equilibrium seems appropriate for the statistical hadronisation approach.

The system created in a relativistic HIC is large enough to be modelled using the Grand Canonical ensemble. This formalism can be used as the central rapidity region is in equilibrium with a thermal reservoir (the rest of the medium created in a HI collision) and quantities like energy, baryon number, charge and isospin are conserved on average. Most of the barrel experiments (as for ALICE central detectors) measure only this part of the phase space, hence the use of the Grand Canonical formalism is allowed. Within this formalism the parameters describing the equilibrium condition of a HIC include the temperature T and the baryon chemical potential μ_B. On this basis the partition function of the system can be written as:

$$Z(T, V, \mu) = \mathrm{Tr}\left[e^{-\beta(H-\Sigma_i Q_i \mu_i)}\right] \tag{1.13}$$

with

$$\mu = \sum_i Q_i \mu_{Q_i} \quad \text{and} \quad \beta = \frac{1}{T} \tag{1.14}$$

where V is the volume of the system at equilibrium, H is the Hamiltonian and μ_{Q_i} is the chemical potential associated to the conserved quantum number Q_i. For a strongly interacting medium, the main conserved quantum numbers are the electric charge Q, the strangeness content of the system S and the baryon number B. The Hamiltonian H in the partition function is that one of a Hadron Resonance Gas since it is able to describe the behaviour of a strongly interacting medium reproducing over a wide temperature range the equation of state obtained with lQCD calculations before the transition to a deconfined state. The choice of the mesonic, baryonic and resonance states included in the Hamiltonian depends on the implementation of the model and it determines the maximum temperature that can be described accurately.

The partition function of the system is the product of the contribution of all the particle states in the Hadron Resonance Gas:

$$Z(T,V,\mu) = \prod_i Z_i(T,V,\mu_i) \quad \rightarrow \quad \log Z(T,V,\mu) = \sum_i \log Z_i(T,V,\mu_i). \tag{1.15}$$

The partition functions are defined by the spin–statistics theorem:

$$\log Z_i(T,V,\mu_i) = \frac{V g_i}{2\pi^2} \int_0^\infty \pm p^2\, dp\, \log\left[1 \pm \lambda_i(T,\mu_i) e^{-\beta\epsilon_i}\right] \tag{1.16}$$

Bose-Einstein distribution for bosons $(+)$ and Fermi-Dirac distribution for fermions $(-)$. The g_i constant is the degeneracy state i and ϵ_i is the energy of one particle of the species i with momentum $p(\epsilon_i = \sqrt{p^2 + m_i^2})$. The dependence on the chemical potentials is encoded within the *fugacity* λ_i:

$$\lambda_i(T,\mu_i) = e^{\beta(B_i\mu_B + S_i\mu_S + Q_i\mu_Q)} = e^{\beta\mu_i} \tag{1.17}$$

where B_i, S_i and Q_i are the baryon number,strangeness content and electric charge associated with the particle species and μ_B , μ_S and μ_Q are the respective chemical potentials. As described in [13], expanding the logarithm and integrating over the momentum, the partition function for the species i becomes:

$$\log Z_i(T,V,\mu_i) = \frac{VTg_i}{2\pi^2} \sum_{k=1}^{\infty} \frac{(\pm 1)^{k+1}}{k^2} \lambda_i^k m_i^2 K_2(\beta k m_i) \tag{1.18}$$

where the $(+)$ is for bosons, the $(-)$ for fermions and the K_2 is the second kind modified Bessel function of second order.

The average number of particle for the species i for a system described by the Gran Canonical ensemble, is defined as:

$$\langle N_i \rangle^{th}(T,V,\mu_i) = \frac{1}{\beta}\frac{\partial}{\partial\mu_i} \log Z_i(T,V,\mu_i) \frac{VTg_i}{2\pi^2} \sum_{k=1}^{\infty} \frac{(\pm 1)^{k+1}}{k} \lambda_i^k m_i^2 K_2(\beta k m_i). \tag{1.19}$$

This equation does not fully describe the particle abundances measured in HI collisions. For the measured yields one should consider the feed–down contributions from all the other particle species (resonances) j in the thermal system that can decay strongly in a final state containing particles of the species i:

$$\langle N_i \rangle^{th}(T,V,\mu) = \langle N_i \rangle^{th}(T,V,\mu_i) + \sum_j \Gamma_{j\rightarrow i} \langle N_j \rangle^{th}(T,V,\mu_j) \tag{1.20}$$

where $\Gamma_{j\rightarrow i}$ is the decay rate of the state j into the final state i.

The definition of particle yields is valid in the limit of a low density system, where the repulsion interaction between the hadrons constituting the systems is negligible.

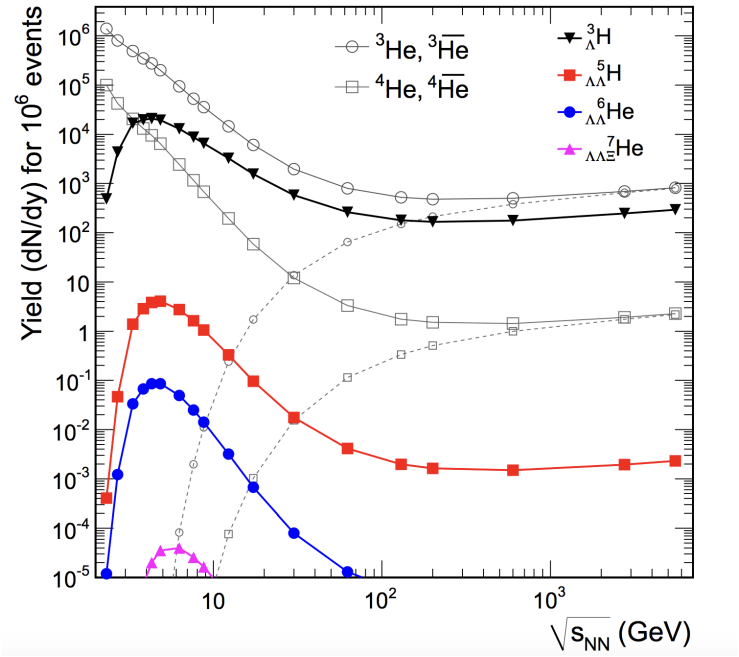

Fig. 1.7: Thermal model predictions for the production of various nuclei, anti-nuclei and hyper–nuclei as a function of the ion collision energy taken from [14]. At low collision energy the baryon chemical potential differs significantly from zero and the particle yield favours matter over anti–matter. As the energy increases, μ_B decreases and this difference vanishes.

The treatment of these interactions is still matter of active theoretical research. Nevertheless Eq 1.20 and 1.19 already indicate the crucial dependencies of the observed particle yields on the temperature T, volume V and the chemical potentials μ_B, μ_Q and μ_S.

Heavy Ions collisions no net strangeness is present in the colliding nuclei, thus $\mu_S = 0$, and μ_Q is fixed by the isospin asymmetry in the collision. Therefore two of the five parameters of the model are constrained by the collisions conditions. The baryon chemical potential μ_B is not constrained as the "amount of baryonic number" transported in the equilibrium region depends on the energy of the collision. The dependence on the volume V of the system can be removed looking at ratio between the yields of different particle species, which therefore depends only on the temperature of the system and on the baryon chemical potential. In the framework of the thermal models, light nuclei yields arise naturally when the chemical freeze–out temperature and the baryon chemical potential are set. A possible explanation on how the light nuclei can survive to the high temperature of the chemical freeze–out was pointed out in [14]: as the system expansion after the chemical freeze–out is supposed to conserve the entropy density, such conservation could be the steering mechanism for the nuclei production. From the fit of the particle abundances at lower energies, the authors of [14] predicted, using the thermal model, the yields of (anti-)nuclei at the LHC energy 1.7.

1.4.2 Coalescence Models

Coalescence models [12] represent a different theoretical approach developed to explain the measured light nuclei production in Heavy Ions collisions. These models address the problem guessing that light nuclei are created at the kinetic freeze-out. They are static models and there is no attempt to give a detailed description of the interactions that lead to their formation. The fundamental idea behind these predictions is that if nuclei constituents are close enough in phase space at the kinematic freeze-out they can bind to form a nucleus. The coalescence models make a prediction about the momentum distribution of the produced light nuclei as a function of the production spectra of the constituents.

The first coalescence model was developed to describe the deuteron formation in proton-nucleus collisions in 1961, in the following years has been extended to the production of various light nuclei in nucleus-nucleus collisions. The momentum spectrum for the i species related is linked to the proton momentum spectrum, which is used as a proxy of the constituent spectrum, by the following equation:

$$E_i \frac{d^3N_i}{dp_i^3} = B_A \Big(E_p \frac{d^3N_p}{dp_p^3} \Big)^A . \tag{1.21}$$

The proton spectrum is assumed to be identical to that one of the constituent neutron. One of the main reasons behind this generalization is that proton spectra are easier to measure in an experiment. These nucleon spectra are not those measured in the experiments, but the ones produced in the collision and not yet modified by the coalescence mechanism. The coalescence parameter B_A is interpreted as a function of the radius p_0, that is the maximum distance at which coalescence can happen. In the simplest formulation of the coalescence models only the momentum space is considered (not the space-time), thus the coalescence parameter can be expressed neglecting the spin:

$$B_A = \Big(\frac{4}{3} \pi \, p_0^3 \Big)^{A-1} \frac{m_i}{m_p^A} . \tag{1.22}$$

where p_0 is the aforementioned radius and m_i and m_p are the nucleus and proton mass, respectively.

More sophisticated versions of this model predict a dependence on the geometry of the system and rely on different constituents momentum spectra and different formulation of the coalescence parameter B_A. Nevertheless, thanks to its simplicity and the presence of just one parameter p_0, the most commonly used for the comparison with the data is the simple model briefly shown above.

Bibliography

1. Gell-Mann, M. A schematic model of baryons and mesons. *Physics Letters* **8,** 214–215 (1964) (cit. on p. 1).
2. Zweig, G. An SU(3) model for strong interaction symmetry and its breaking. *Developments In The Quark Theory Of Hadrons* **1** (1964) (cit. on p. 1).
3. Zweig, G. An SU(3) model for strong interaction symmetry and its breaking II. *Developments In The Quark Theory Of Hadrons* **1** (1964) (cit. on p. 1).
4. Fritzsch, H. & Gell-Mann, M. Current Algebra: Quarks and What Else? *Proceedings of the XVI International Conference on High Energy Physics* **2,** 135 (1972) (cit. on p. 2).
5. Fritzsch, H. & ans Heinrich Leutwyler, M. G.-M. Advantages of the color octet gluon picture. *Physics Letters B* **47,** 365–368 (1973) (cit. on p. 2).
6. Tanabashi, M., Hagiwara, K., Hikasa, K., *et al.* Review of Particle Physics. *Physical Review D* **98,** 030001 (3 2018) (cit. on pp. 3, 4).
7. Wilson, K. G. Confinement of quarks. *Physical Review D* **10,** 2445–2459 (8 1974) (cit. on p. 3).
8. Braun-Munzinger, P., Koch, V., Schäfer, T. & Stachel, J. Properties of hot and dense matter from relativistic heavy ion collisions. *Physics Reports* **621.** Memorial Volume in Honor of Gerald E. Brown, 76–126 (2016) (cit. on p. 5).
9. Alford, M. G., Schmitt, A., Rajagopal, K. & Schäfer, T. Color superconductivity in dense quark matter. *Reviews of Modern Physics* **80,** 1455–1515 (4 2008) (cit. on p. 5).
10. Miller, M. L., Reygers, K., Sanders, S. J. & Steinberg, P. Glauber modeling in high energy nuclear collisions. *Ann. Rev. Nucl. Part. Sci.* **57,** 205–243 (2007) (cit. on pp. 6, 7).
11. Gale, C., Jeon, S. & Schenke, B. Hydrodynamic Modelling og Heavy-Hion Collisions. *International Journal of Modern Physics A* **28,** 1340011 (2013) (cit. on p. 9).
12. Kapusta, J. I. Mechanisms for deuteron production in relativistic nuclear collisions. *Physical Review C* **21,** 1301–1310 (4 1980) (cit. on pp. 10, 14).
13. Braun-Munzinger, P., Redlich, K. & Stachel, J. Particle production in heavy ion collisions, 491–599 (2003) (cit. on p. 12).
14. Andronic, A., Braun-Munzinger, P., Stachel, J. & Stocker, H. Production of light nuclei, hypernuclei and their antiparticles in relativistic nuclear collisions. *Physical Letters* **B697,** 203–207 (2011) (cit. on p. 13).